



Deposited via The University of Leeds.

White Rose Research Online URL for this paper:

<https://eprints.whiterose.ac.uk/id/eprint/144461/>

Version: Accepted Version

Proceedings Paper:

Ren, Z, Zhou, C, Xin, S et al. (2017) HERI hand: A quasi dexterous and powerful hand with asymmetrical finger dimensions and under actuation. In: 2017 IEEE/RSJ International Conference on Intelligent Robots and Systems (IROS). 2017 IEEE/RSJ (IROS), 24-28 Sep 2017, Vancouver, BC, Canada. IEEE, pp. 322-328. ISBN: 978-1-5386-2682-5. ISSN: 2153-0858. EISSN: 2153-0866.

<https://doi.org/10.1109/IROS.2017.8202175>

© 2017 IEEE. Personal use of this material is permitted. Permission from IEEE must be obtained for all other uses, in any current or future media, including reprinting/republishing this material for advertising or promotional purposes, creating new collective works, for resale or redistribution to servers or lists, or reuse of any copyrighted component of this work in other works.

Reuse

Items deposited in White Rose Research Online are protected by copyright, with all rights reserved unless indicated otherwise. They may be downloaded and/or printed for private study, or other acts as permitted by national copyright laws. The publisher or other rights holders may allow further reproduction and re-use of the full text version. This is indicated by the licence information on the White Rose Research Online record for the item.

Takedown

If you consider content in White Rose Research Online to be in breach of UK law, please notify us by emailing eprints@whiterose.ac.uk including the URL of the record and the reason for the withdrawal request.

HERI Hand: A Quasi Dexterous and Powerful Hand with Asymmetrical Finger Dimensions and Under Actuation

Zeyu Ren, Chengxu Zhou, Songyan Xin, Nikos Tsagarakis

Abstract—In this paper, the Hardware Embedded Reduced Intricacy (HERI) Hand, which is a novel tendon driven three-finger under-actuated hand demonstrating balanced dexterous finger manipulation and powerful grasping of common objects is presented. The third finger of HERI Hand is asymmetrically designed in terms of dimensions to emulate the functionality for combining middle finger, ring finger and little finger of a human hand. HERI Hand is equipped with three actuators devoted to the actuation of the flexion of the index finger and thumb, the flexion of the third finger and finally the thumb abduction and adduction motion with the latest drive having no interference with other transmissions. The proposed hand is capable of realizing delicate finger manipulation such as opening a lidded cup, which is super suitable to accomplish in such configuration. At the same time the hand demonstrates high grasping strength capacity thanks to the actuation sizing permitted by the under-actuated configuration. The hand is also equipped with tactile/pressure sensors distributed in the phalanges, which leaves open the possibility of potential applications for sophisticated finger manipulations taking into account the phalanges contact forces. Three different sets of experiments were carried out to demonstrate the performance of HERI Hand and validated its functionality.

I. INTRODUCTION

In the past few decades, many multi-fingered robotic hands have been developed for both dexterous and robust grasping. Mainly, they can be classified into two categories, fully-actuated and under-actuated hands. Fully-actuated hands, such as UTAH/M.I.T Hand [1], DLR Hand [2], Robonaut 2 Hand [3] and DEXMART Hand [4] etc., are capable of controlling each finger joint independently, thus they are able to mimic most of the sophisticated human hand motions by well-designed control strategies. Meanwhile, their superior capabilities also introduce challenges into the hardware and control designing stage, such as limited space for dozens of actuators, demanding algorithm development due to the redundancy, as well as the concomitant reliability issues and high costs. Therefore, making trade-offs between the actuator quantity and dexterity has been attracting attentions to this end, which flourishes the developments of under-actuated hands, such as RTR II Hand [5], MANUS-HAND [6], Barrett Hand [7], SDM Hand [8], Colombia Hand [9], Ritsumeikan robotic hand [10] and Pisa/IIT SoftHand [11] etc.

The aforementioned different types of the under-actuated hands have made greatly progress in terms of anthropomorphic design, dexterous grasping, robust holding, sensor feedback control as well as the low-cost yet robust hardware

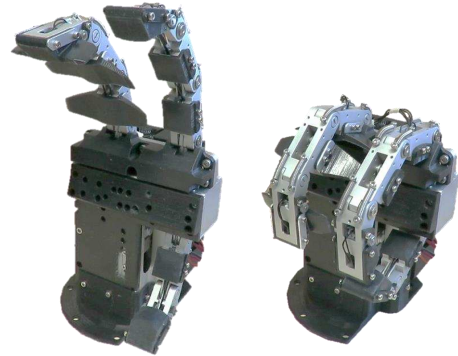


Fig. 1: Open and close posture of the proposed three-finger under-actuated HERI Hand.

design. Nevertheless, it is hard for an under-actuated hand to possess all the above-mentioned advantages simultaneously. For instance, Pisa/IIT SoftHand [11] is designed with perfect anthropomorphism, superior robustness and excellent self-protection property thanks to its novel compliant structures. However, due to its inherent single-actuator-driven characteristic, dexterous finger manipulation performance would be negatively effected. Ritsumeikan robotic hand [10] is able to achieve pinch, lateral pinch motions and powerful anthropomorphic grasping efficiently with three independent actuators and one solenoid for locking mechanism. However, the deficient in embedded sensors limits its capability in delicate sensitive finger manipulation.

Given this situation, we are motivated to design an under-actuated hand which is competent in both dexterous and powerful hand manipulation, and meanwhile equipped with sufficient sensors for potential applications utilizing contact force information. Moreover, it should be driven by as few actuators as possible taking into account simplifying design mechanically and reducing cost at the precondition of not losing dexterity. Furthermore, this hand will be mounted on a human-sized robot and a Centaur-like robot [12] which are specially developed for disaster response, hence it should be capable of certain level of dexterous manipulation as well as powerful grasping for manipulated objects in such environment. Lastly, its general dimension should be similar as a human hand in order to manipulate the tools designed for human. As a result, we developed the Hardware Embedded Reduced Intricacy (HERI) Hand, which is a three-finger under-actuated hand as shown in Fig. 1.

The rest of this paper is organized as follows. Section II reviews the design principle of quantity and distribution

arrangement for fingers and actuators. Section III details the mechanical design and hardware description. In Section IV, three sets of experiments were carried out to demonstrate the performance of HERI Hand. In Section V, summary and prospect for the work are presented.

II. DESIGN SCHEME

For achieving the aforementioned requirements, the main hand characteristics in terms of fingers and degree of actuations (DoAs) configurations are determined in this section.

A. Finger Quantity and Distribution

Among the existing under-actuated hands, there are mainly three different designs in terms of finger quantity, which are

(i) five-finger hands, (ii) four-finger hands and (iii) three-finger hands.

Several examples for each type are as follows,

- (i) Ritsumeikan robotic hand [10], Pisa/IIT SoftHand [11],
- (ii) Yale OpenHand Model T [13],
- (iii) RTR II [5], SPRING Hand [14], Barrett Hand [7].

However, by analyzing the grip taxonomy [15], which is a thorough investigation for tool usage habit of hands, one could find that in the majority of powerful grasps performed by the human, the middle finger, ring finger and little finger usually wrap around the object all together in a coordinated manner. Therefore, they can be considered as single Virtual Finger [16] for these grasp tasks and thus inspired us to simplify the hand design by combining the last three fingers' main functionalities into only one finger, which naturally leads to type (iii). As a result, the three-finger type was chosen as the finger quantity design of HERI Hand.

In addition, according to the study of human multi-finger force production [17], the coupled motion of last three fingers has the smallest Enslaving Effect among others, which means that combining them together will affect less to other fingers' motion. Therefore, imitatively constructing the third finger of HERI Hand by bundling up the last three fingers of human hands is also a reasonable simplification from the biomechanics point of view. The humanoid robot HRP-3 [18] and the five-fingered assistive hand [19] adopted a similar design of a three-finger-combined into one third finger.

To provide larger contact area while at the same time permitting the third combined finger to conform to the object surface along the lateral direction, three wide rubber patches are mounted on phalanxes of the third finger to triple the contact surface, which directly reflects the asymmetrical dimension property of this finger with respect to the index finger and the thumb. This enables the adoption of the contact area of the combined third finger replicating the flexibility produced by the ring and little fingers.

Therefore, as shown in Fig. 1, HERI Hand equips with three fingers: the third finger (combining the middle, ring and little fingers), the index finger and the thumb. The thumb is placed oppositely to the index finger to simplify the mechanical design for the realization of pinch motion. Additionally, two rubber-made compliant structures are mounted at the bases of index finger and third finger to avoid the finger

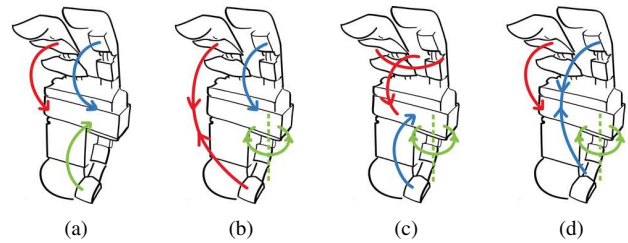


Fig. 2: Possible proposals for assigning DoA to the three-finger under-actuated hand.

structure damage caused by unexpected lateral impacts in the direction of joints rotation axis.

B. Degree of Actuation Assignment

As the finger quantity and distribution are decided, it comes into the issue for DoA configurations selection. For the purpose of simplifying the mechanical structure, reducing the cost, and meanwhile maintaining the finger manipulation capabilities to the greatest extent, we finally set the DoA quantity to be three. Fig. 2 depicts four possible proposals of the potential three-DoA under-actuation configuration for the desired hand. Fig. 2(a) provides independent flexion for each finger but lacks the thumb rotation, which will limit the hand's dexterous manipulation performance; Fig. 2(b) possesses one kind of unhuman-like grasping motion, namely the combined motion for third finger and thumb but simultaneously allows for independent index flexion motion that can be useful to perform triggering actions e.g. switching on powerful tools; Fig. 2(c) merges the motion of index and third finger, which may interfere with each other in some cases where a precision grasp such as palmar pinch is necessary. Fig. 2(d) provides the independent flexion motion for third finger, combined flexion motion for index finger and thumb as well as the independent thumb rotation motion.

In summary, options (a) and (c) were excluded as they do not demonstrate any specific advantages with respect to the other two. Under-actuation arrangements (b) and (d) provide very similar functionality in terms of robustness and dexterity as well as have both pros and cons with respect to each other. They could be both selected depending on the choice of the dexterity feature to be highlighted that is the independent index trigger action provided by configuration (b) or the natural index/thumb pitch feature permitted by configuration (d). In this first prototype our choice target was to permit the execution of natural index/thumb pitch action and for this reason configuration (d) was selected in Table I, which presents the significant DoA assignment specifically.

DoA₁ will mainly contribute to the powerful grasping, while DoA₂ and DoA₃ will undertake precise natural pinching and dexterous manipulation, which presents the property for asymmetrical actuation. A special consideration needs to be taken for DoA₂, if either index finger or thumb is stuck by the object during practical grasping, the other finger should be capable of continuously executing the desired motion. Besides, DoA₃ should be independent with DoA₂,

TABLE I: DoA assignment of HERI Hand.

	DoA ₁	DoA ₂	DoA ₃
Motion Description	Third finger flexion motion	Index finger and thumb combined flexion motion	Thumb rotation

TABLE II: Value for finger phalanx geometry parameters.

[mm]	l	l _c	a	b	c	d	r _p	r _j	r _m
Body phalanx	40	-	14	3.5	26	-	1.5	9	3.5
Tip phalanx	-	28	-	-	-	20	-	-	-

that means no coupled motions should exist for the thumb rotation to permit the deterministic placement and control of the thumb opposition.

III. DESIGN SPECIFICATIONS

In this section, the design details of HERI Hand in terms of finger kinematics analysis and design, actuator selection, tendon route arrangement as well as the finger sensors configuration are presented to further introduce the proposed under-actuated hand.

A. Finger Design

Similarly as the human fingers, we consider three phalanxes for the index and third finger whereas for the thumb only two are utilized. With the consideration of reducing fabrication cost and maintenance time, interchangeable and simplification are adopted as two essential principles for the phalanx design. As a result, there are only two types of phalanx modules for all fingers, named body phalanx and tip phalanx, as shown in Fig. 3(a) and Fig. 3(b). Therefore, totally five body phalanxes and three tip phalanxes are used for constructing the three fingers of the hand and their dimensions are decided based on approximately the same size of a normal adult human hand, taking into account the workspace for grasping common objects, utilizing human tools as well as the size of the robot that the hand will be mounted on.

Since the classic *Da Vinci's Mechanism* [20, p. 55] is adopted as the transmission approach for the under-actuated finger flexion motion, the same pulley layout plan is also followed for each phalanx. Note that, the torque distribution for each joint is realized by the springs with proper stiffness placed at the corresponding joints, despite the fact that the pulley layouts are the same for every body phalanx. Finally, each body and tip phalanx are equipped with the tactile sensor placed in the middle phalanx position. As an example, the detailed geometry dimensions of the third finger are depicted in Fig. 3(c) and the values are shown in Table II.

B. Actuator Specification Selection

The strength of the under-actuated finger in terms of ability to exert a certain grasping force is closely related to the capabilities of its actuator. It is therefore essential to select the specification of the motor carefully to ensure enough grasping force tolerance under the severest designed circumstance. In this section, the actuation specification

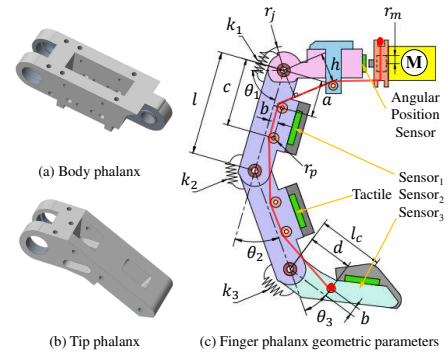


Fig. 3: Finger phalanx type and geometric parameters.

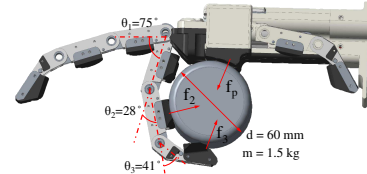


Fig. 4: Top view for grasping desired object in vertical.

selection process of DoA₁, which is intended for powerful grasping, is detailed as an example. Similar approach is taken for selecting the actuator driving the flexion motion of index and thumb (DoA₂) to satisfy the design requirements and meantime follow the design principles defined in III-A.

Fig. 4 presents the severest grasping scenario in which only the DoA₁ is required to keep grasping the object. This scenario is designed with the hand holding a cylindrical object horizontally to the gravity. Therefore only the friction force is utilized for holding the object, which means that there is no extra contact points except the vertical surface of phalanxes and the palm. The cylindrical object has a diameter of 60 mm and a mass of 1.5 kg, which is considered as a cylindrical tool that HERI Hand could handle in this situation. As Fig. 4 shows, only the middle phalanx, distal phalanx and palm will make contacts with the object in this size and profile, generating the vertical contact forces as f_2 , f_3 and f_p respectively. The angles of the finger joints under this grasping scenario can be easily evaluated as $\theta_1 = 75^\circ$, $\theta_2 = 28^\circ$, $\theta_3 = 41^\circ$.

In general cases which are not only limited in Fig. 4 scenario, the output motor torque τ_m under a certain posture with contact forces on the phalanxes can be written as

$$\tau_m = (\mathbf{J}^T \mathbf{F} + \tau_k) \cdot \frac{r_m}{h} \cdot \frac{1}{\eta_m \eta_t} \quad (1)$$

where

$$\mathbf{J} = \begin{bmatrix} l/2 \\ l/2 + l \cdot \cos \theta_2 \\ l_c + l \cdot \cos(\theta_2 + \theta_3) + l \cdot \cos \theta_3 \end{bmatrix} \quad (2)$$

functions as Jacobian Matrix \mathbf{J} ,

$$\mathbf{F} = [f_1 \quad f_2 \quad f_3]^T \quad (3)$$

contains the vertical contact forces exerted at the proximal, middle and distal phalanx, respectively.

$$\tau_k = (k_1\theta_1 + k_2\theta_2 + k_3\theta_3) \cdot r_j^2 \quad (4)$$

is the sum of the torques generated by the spring deflection on each joint. k_1 , k_2 and k_3 are the stiffnesses of the corresponding returning spring connected between two phalanxes at three finger joints, as shown in Fig. 3(c). r_j is the distance between the joint rotation center to the corresponding spring and r_m is the radius of the motor output gear. h is the tendon force arm at the first finger joint and dependency with θ_1 , which can be obtained from geometry calculation at a certain finger posture. η_m and η_t are the motor efficiency and tendon transmission efficiency respectively.

Each spring stiffness is defined as follows, $k_1 = 230$ N/m, $k_2 = 440$ N/m and $k_3 = 740$ N/m, which are decided by two constrains. The first is for eliminating the joint deflection caused by the phalanx gravity when the palm facing the ground, which determines the minimum value of k_1 for ensuring the robustness property meanwhile. The second is to avoid the finger *Roll-Back Phenomenon* [20, p. 49], which normally happens during a continuous finger closing motion, that the last phalanx slides against the object resulted in a situation that the finger grasps nothing but itself, which decides the specific ratio between k_1 , k_2 and k_3 .

As a result, we could utilize (1) to calculate the minimum output torque of DoA₁ actuator under the severest single third finger grasping scenario shown in Fig. 4. The efficiency coefficients η_m and η_t will be reasonable set for practically estimating the real working conditions. The vertical contact forces f_2 , f_3 and f_p in Fig. 4 satisfy the relation with the object's gravity in the critical condition where sliding friction would occur, which as following,

$$m \cdot g = \mu \cdot (f_2 + f_3 + f_p) \quad (5)$$

where $m = 1.5$ kg is the cylinder's weight, $g = 9.81$ m/s² is the gravitational constant, $\mu = 0.4$ is the static frictional coefficient between the object and the phalanx rubber.

Fig. 5 shows the corresponding motor torque τ_a , which depends on different contact forces f_2 and f_3 distributions. The white curve, whose maximum torque is 0.76 Nm, represents the minimum motor torque which demanded for holding a 1.5 kg cylinder under the critical condition in every different f_2 and f_3 distribution. We finally choose Maxon EC-Max 22 motor for its compact size and adequate torque output, which is 1.2 Nm and presented as transparent green plane in Fig. 5. The desired motor torque suffices the initial design requirements obviously and meanwhile possesses the maximum capacity to theoretically hold a 2.7 kg cylinder.

C. Tendon Route Description

The main mechanical transmission systems between actuators and end-effectors of DoA₁ and DoA₂ are tendon based. The tendon routing design of HERI Hand is significant for achieving grasping performance and mechanical transmission in high efficiency. The *Dacron* rope is used as

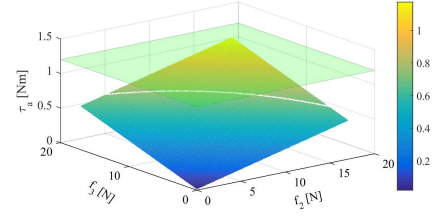


Fig. 5: Minimum required motor torque τ_a under different contact force combinations.

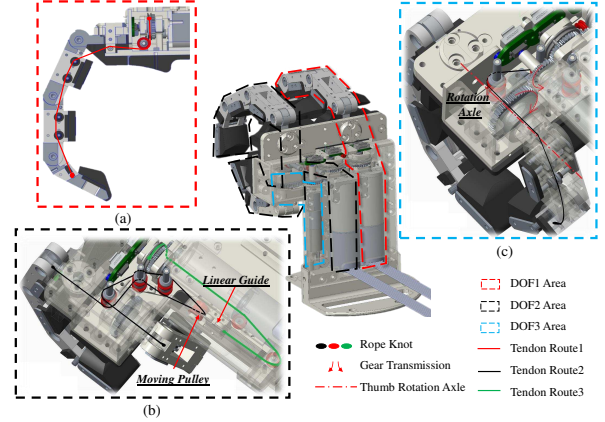


Fig. 6: Tendon route for driving corresponding DoA.

the specific tendon material for its high strength and wear resistance properties.

As shown in Fig. 6(a), the tendon route depicted in red is designed for DoA₁, namely the powerful grasping of the third finger. It is based on the classical *Da Vinci's Mechanism* [20, p. 55] which uses multiple pulleys supported by miniature bearings to significantly decrease the friction between the tendon and the mechanical parts. This sliding friction reduction as well as the short tendon route distance enable DoA₁ to efficiently generate grasping forces.

DoA₂, which is dedicated to the combined flexion motion of index finger and thumb, additional attention was given to ensure its efficient transmission. Its tendon route is combined by two segments as shown in Fig. 6(b), the green tendon route is the main route connected with DoA₂ motor and then divided into two black branch routes fixed with the tips of thumb and index finger respectively, directly after a *Linear Guide* and a *Movable Pulley* that implement a differential tendon mechanism between the motions of the index and the thumb which allowing either finger to continue its flexion motion even if the other finger is constrained. However, driving two under-actuated fingers by only one actuator increases the sliding friction between tendon and mechanism due to the complicated tendon route and meanwhile may cause the coupling mechanism's slack issue. For addressing these aforementioned issues, additional pulleys (17 in total) supported by bearings including the essential *Movable Pulley* were used to reduce friction, the slack issue is simultaneously solved by the low tendon friction as well as the pretension force generated by the finger joint springs.

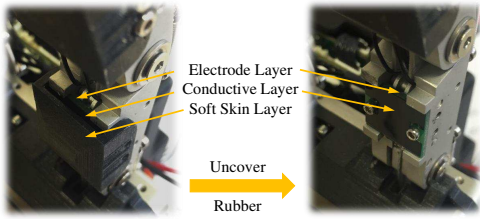


Fig. 7: Three individual layers for each tactile sensor.

DoA₁ transmission is more efficient and can generate higher grasping forces than DoA₂ based on the simple fact that the driving force of DoA₂ is divided for two under-actuated fingers, despite that the two actuators are of the same specification. This asymmetry in the two transmission systems inherently distributes the power grasp functionality to the third finger rather than to the index one.

DoA₃, which is responsible for the thumb rotation, is directly driven by a reliable two-gear transmission as shown in Fig. 6(c). It should be independent of DoA₂ and not interfere with the thumb flexion motion, which means that there should not be any displacement for the thumb tendon when it rotates. To achieve this decoupling, the thumb flexion tendon is routed through the center axis of the thumb rotation joint.

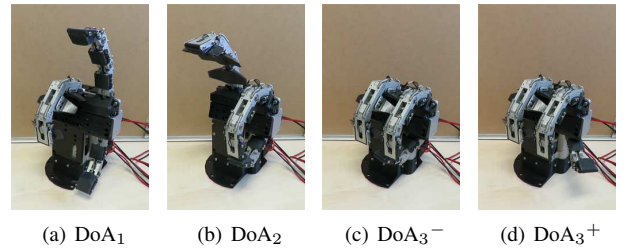
In conclusion, after the discussion in III-B and III-C, the final configuration for each DoA actuation components and the corresponding finger grasp forces are shown in Table III.

D. Sensor Configuration

Receiving sensory feedback information during finger manipulations is beneficial for interactive finger motion control. HERI Hand is equipped with two types of sensors, namely the three absolute angular position sensors for each motor of the independent DoA and the eight tactile sensors in total, which are placed respectively under the elastic rubber layer on each phalanx as shown in Fig. 3(c) and Fig. 7.

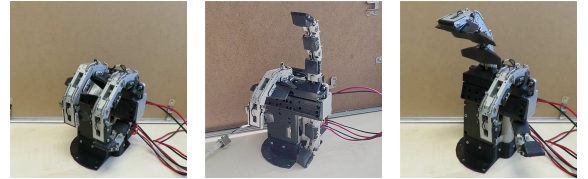
The absolute angular position sensor utilized is AS5048A from *ams AG*, which is a 14 bit absolute position sensor providing an angle measurement resolution of 0.022 degrees. However for DoA₁ and DoA₂, only the tendon displacement can be estimated by multiplying the angular position sensor feedback angle with the motor tendon pulley radius, while the exact position of each finger phalanx remains unknown due to the properties of under-actuated finger.

The tactile/contact pressure sensors are specially customized sensors developed using a resistive sensing principle. They are composed by an customized electrode layer, a resistive/conductive layer, and a soft skin top layer as shown in Fig. 7. The vertical component of the external force applied to the phalanxes can be measured by using the resistance change of the sensors after the basic calibration process by vertically placing one 100 g weight above on each of them. The maximum accuracy for the utilized pressure sensor can reach 0.08N.



(a) DoA₁ (b) DoA₂ (c) DoA₃⁻ (d) DoA₃⁺

Fig. 8: Independent motion of one DoA description.



(a) DoA₁ and DoA₂ (b) DoA₁ and DoA₃ (c) DoA₂ and DoA₃

Fig. 9: Coordinated motion of two DoAs description.

IV. EXPERIMENTAL EVALUATION

To verify the effectiveness of HERI Hand, mainly three different sets of experiments were carried out in this section to demonstrate the hand's performance in terms of independent/combined DoAs motions, dexterous manipulations and robust grasping.

A. DoA Motion Verification

As presented in Section II, each individual DoA is designed not to interfere with other DoAs. Therefore it is necessary to firstly demonstrate the finger motions using different combinations of DoAs. Another purpose of the first experiment is to analysis whether these under-actuated fingers are reasonably designed to be able to avoid the negative *Roll-Back Phenomenon*.

Fig. 8 shows the independent motion of each DoA, namely Fig. 8(a) and Fig. 8(b) demonstrate the flexion motions of DoA₁ and DoA₂ respectively, Fig. 8(c) and Fig. 8(d) present the thumb rotation motion while all the fingers were closed. Actually Fig. 8(c) and Fig. 8(d) also show the combination motions of all the three DoAs simultaneously. In fact, the thumb rotation motion (DoA₃) could barely undertake a practical manipulation individually, rather contributes as an auxiliary to coordinated motions with other DoAs, an application is presented in the next experiment. Fig. 9 demonstrates the coordinated motions of utilizing two DoAs in different combinations, respectively.

As a proof of concept, this experiment verified the independent motions of DoAs which has shown the effectiveness of the original design intentions. Especially, no interference was observed during the motions of DoA₂ and DoA₃ thanks to the aligning of the thumb tendon and the thumb rotation axis. Besides, each phalanx on under-actuated finger is driven to close at an appropriate order, which proves the finger design fully prevents the occur for negative *Roll-Back Phenomenon*.

TABLE III: Configuration for each DoA actuation components and expected finger grasp forces.

	DoA ₁	DoA ₂	DoA ₃
Motor Type	EC-Max 22, Brushless, Hall sensors, Maxon ^{*(1)}	1218A, Brushless-DC, FAULHABER ^{*(2)}	
Gearbox Type	Planetary Gearhead GP 22 C, Maxon	Planetary Gearhead 12-4, FAULHABER	
Gearbox Ratio		104:1	256:1
Continuous Torque		1.2 Nm	0.3 Nm
Peak Torque		1.9 Nm	0.45 Nm
Estimated Transmission Efficiency ^{*(3)}	0.44	0.36	0.5
Tendon Transmission Length	145 mm	348mm & 189mm ^{*(4)}	-
Number of tendon transmission pulleys	6	17	-
Expected Continuous Grasp Force ^{*(5)}	17 N	10 N	-
Expected Peak Grasp Force ^{*(6)}	27 N	15.8N	-

Note: ^{*(1)}: The selected motor for DoA₁ is powerful enough for DoA₂, for interchangeable principle, the same type was adopted; ^{*(2)}: This motor is selected mainly due to its compact size and appropriate reduction ratio for DoA₃; ^{*(3)}: This is the final efficiency including both the motor efficiency and the tendon transmission efficiency; ^{*(4)}: 348 mm and 189 mm are the length for tendon in black and green respectively, as shown in Fig. 6; ^{*(5)–(6)}: This is the force generated from the end-effector phalanx, namely the distal phalanx on corresponding finger.

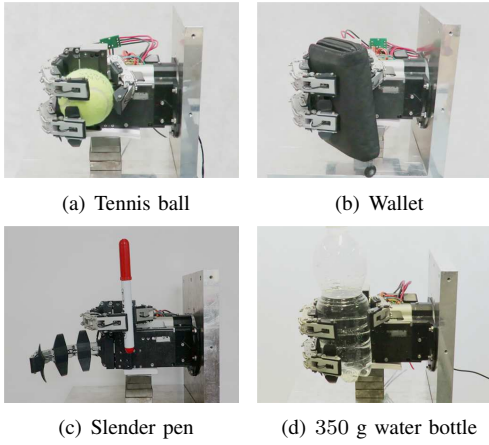


Fig. 10: Versatile grasp on daily common objects.

B. Dexterous Manipulation Demonstration

In the second experiment, the dexterous grasp validations were firstly performed on several daily used objects to demonstrate the versatility of the hand. Some grasping examples are shown in Fig. 10, a spherical tennis ball, a irregular shape wallet, a slender pen as well as a plastic bottle of 350 g water were initially placed in the hand by human and then firmly grasped by the robotic hand. All the grasping tests were performed more than one minute with the objects securely held by the hand.

Furthermore, for the purpose of fully taking advantage of all the equipped DoAs on the hand, a more challenging task involving a certain level of dexterity by executing opening a cup with a hinged lid was carried out. Fig. 11 shows this finger manipulation by simultaneously using three DoAs of the hand. The cup was firstly placed by the human operator and then grasped using both the DoA₁ and DoA₂ as Fig. 11(a) shows. After all the three fingers closed firmly to hold the cup, the thumb was commanded independently to rotate outwards, therefore pushed the lid to open, as shown in Fig. 11(b) and finally it rotated back to resume grasping the cup, which is presented in Fig. 11(c).

Fig. 12(a) and Fig. 12(b) present the tactile and position

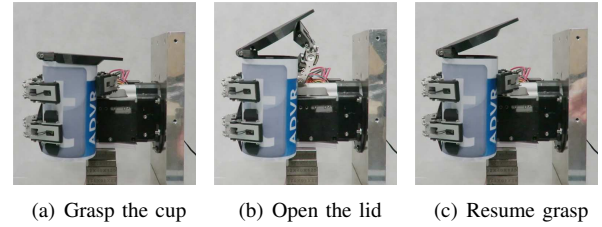


Fig. 11: Process for opening a lidded cup utilizing all the three DoAs of HERI Hand simultaneously.

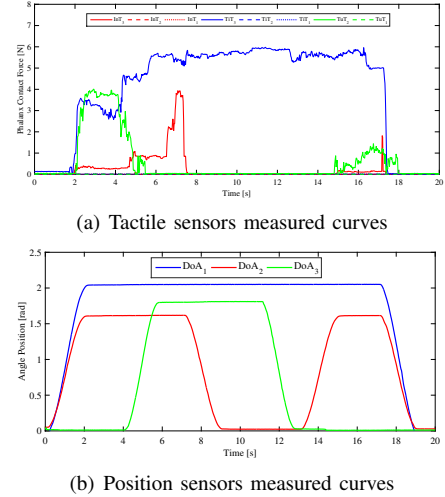
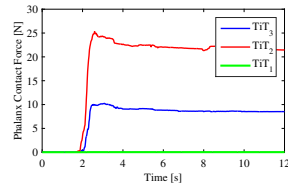
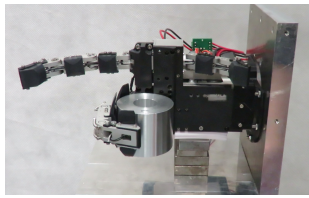


Fig. 12: Sensors measured curves for opening bottle lid.

sensors measured curves correspondingly during the whole manipulation process for opening lid. The label in Fig. 12(a) need to be explained as following, the measured curves for tactile sensors on index finger are abbreviated as InT , similarly TiT and TuT are respectively for the curves measured on the third finger and the thumb, and their specific number orders in subscript are shown in Fig. 3.

C. Robust Grasp Demonstration

The third finger of HERI Hand is specially designed for powerful grasping. The third experiment was therefore



(a) Grasp of a 500 g metal sleeve (b) Tactile sensors measured curves

Fig. 13: Third finger robust grasp demonstration.

carried out to verify the robustness of this third finger for heavy object grasping. Similarly to the previous experiments, the hand was fixed to a metal base horizontally. This meant that the object could be only grasped vertically, therefore the supporting forces provided by the hand coming solely from the static frictions between the phalanxes and the object, unlike as other configurations which the object could be supported by the structure of the hand, on the palm or fingers for instance. This experiment setup could be considered as the severest situation for demonstrating the grasp robustness.

For this reason, a 50 mm diameter metal sleeve weighted 500 g was used to test the third finger's grasp robustness. As shown in Fig. 13, the metal sleeve was firmly grasped by only the third finger and held for more than one minute. The first 12 seconds for the third finger's tactile sensors measured curves are plotted in Fig. 13(b). One can observe that, with the grasping configuration as shown in Fig. 13(a), only the distal and middle phalanx had the contacts with the object during the grasp, and the maximum contact force of 25.4 N was applied at the middle phalanx when the object was initial firmly grasped.

V. CONCLUSION

This paper presents the design philosophy of a novel tendon driven three-finger under-actuated HERI Hand in terms of finger configurations and actuation arrangements. Meanwhile, the mechanical design specifications for achieving the desired functionalities are detailed as well. The novel two continuous coupling motions of the thumb and the asymmetrical geometric structure of the fingers are the main contributions to the research community of designing under-actuated hands of high functionality. The dexterous and powerful manipulation performance of HERI Hand were demonstrated by series of experiments based on the delicate control utilizing the tactile and position sensory feedback.

Concerning the future work, HERI Hand will be mounted on a Centaur-like robot [12] after necessary modification and improvement in mechanism. More efforts will be paid to the development of intelligent controllers which will fully utilize the existing sensors for dexterous manipulations, such as under-actuated finger configuration estimation, object properties measurement and compliant finger interaction.

ACKNOWLEDGMENT

This work is supported by the European Union's Horizon 2020 robotics program CENTAURO (ICT-23-2014, 644839)

and CogIMon (ICT-23-2014, 644727). The author would also like to thank Phil Edward Hudson and Alessio Margan for their great support in electronics and embedded control.

REFERENCES

- [1] S. C. Jacobsen, J. E. Wood, D. Knutti, and K. B. Biggers, "The UTAH/MIT dextrous hand: Work in progress," *The International Journal of Robotics Research*, vol. 3, no. 4, pp. 21–50, 1984.
- [2] M. Grebenstein, M. Chalon, G. Hirzinger, and R. Siegwart, "Antagonistically driven finger design for the anthropomorphic DLR hand arm system," in *IEEE-RAS International Conference on Humanoid Robots*, 2010, pp. 609–616.
- [3] M. A. Diftler, J. Mehling, M. E. Abdallah, N. A. Radford, L. B. Bridgwater, A. M. Sanders, R. S. Askew, D. M. Linn, J. D. Yamokoski, F. Permenter *et al.*, "Robonaut 2—the first humanoid robot in space," in *IEEE International Conference on Robotics and Automation*, 2011, pp. 2178–2183.
- [4] G. Palli, C. Melchiorri, G. Vassura, U. Scarcia, L. Moriello, G. Berselli, A. Cavallo, G. De Maria, C. Natale, S. Pirozzi *et al.*, "The DEXMART hand: Mechatronic design and experimental evaluation of synergy-based control for human-like grasping," *The International Journal of Robotics Research*, vol. 33, no. 5, pp. 799–824, 2014.
- [5] B. Massa, S. Roccella, M. C. Carrozza, and P. Dario, "Design and development of an underactuated prosthetic hand," in *IEEE International Conference on Robotics and Automation*, 2002, pp. 3374–3379.
- [6] J. Pons, E. Rocon, R. Ceres, D. Reynaerts, B. Saro, S. Levin, and W. Van Moorleghem, "The MANUS-HAND dextrous robotics upper limb prosthesis: mechanical and manipulation aspects," *Autonomous Robots*, vol. 16, no. 2, pp. 143–163, 2004.
- [7] A. Edsinger-Gonzales, "Design of a compliant and force sensing hand for a humanoid robot," DTIC Document, Tech. Rep., 2005.
- [8] A. M. Dollar and R. D. Howe, "The highly adaptive SDM hand: Design and performance evaluation," *The international journal of robotics research*, vol. 29, no. 5, pp. 585–597, 2010.
- [9] L. Wang, J. DelPreto, S. Bhattacharyya, J. Weisz, and P. K. Allen, "A highly-underactuated robotic hand with force and joint angle sensors," in *IEEE/RSJ International Conference on Intelligent Robots and Systems*, 2011, pp. 1380–1385.
- [10] K. Mitsui, R. Ozawa, and T. Kou, "An under-actuated robotic hand for multiple grasps," in *IEEE/RSJ International Conference on Intelligent Robots and Systems*, 2013, pp. 5475–5480.
- [11] M. G. Catalano, G. Grioli, E. Farnioli, A. Serio, C. Piazza, and A. Bicchi, "Adaptive synergies for the design and control of the Pisa/IIT soft-hand," *The International Journal of Robotics Research*, vol. 33, no. 5, pp. 768–782, 2014.
- [12] L. Baccelliere, N. Kashiri, L. Muratore, A. Laurenzi, M. Kamedula, A. Margan, S. Cordasco, J. Malzahn, and N. G. Tsagarakis, "Development of a human size and strength compatible bi-manual platform for realistic heavy manipulation tasks," in *IEEE/RSJ International Conference on Intelligent Robots and Systems*, 2017.
- [13] R. R. Ma, L. U. Odhner, and A. M. Dollar, "A modular, open-source 3d printed underactuated hand," in *IEEE International Conference on Robotics and Automation*, 2013, pp. 2737–2743.
- [14] M. C. Carrozza, C. Suppo, F. Sebastiani, B. Massa, F. Vecchi, R. Lazzarini, M. R. Cutkosky, and P. Dario, "The SPRING hand: development of a self-adaptive prosthesis for restoring natural grasping," *Autonomous Robots*, vol. 16, no. 2, pp. 125–141, 2004.
- [15] M. Cutkosky and P. Wright, "Modeling manufacturing grips and correlations with the design of robotic hands," in *IEEE International Conference on Robotics and Automation*, 1986, pp. 1533–1539.
- [16] M. A. Arbib, "Coordinated control programs for movements of the hand," *Hand function and the neocortex*, pp. 111–129, 1985.
- [17] V. M. Zatsiorsky, Z.-M. Li, and M. L. Latash, "Enslaving effects in multi-finger force production," *Experimental brain research*, vol. 131, no. 2, pp. 187–195, 2000.
- [18] K. Kaneko, K. Harada, F. Kanehiro, G. Miyamori, and K. Akachi, "Humanoid robot HRP-3," in *IEEE/RSJ International Conference on Intelligent Robots and Systems*, 2008, pp. 2471–2478.
- [19] Y. Hasegawa, Y. Mikami, K. Watanabe, and Y. Sankai, "Five-fingered assistive hand with mechanical compliance of human finger," in *IEEE International Conference on Robotics and Automation*, 2008, pp. 718–724.
- [20] L. Birglen, T. Laliberté, and C. M. Gosselin, *Underactuated robotic hands*. Springer, 2007, vol. 40.